Noname manuscript No.
(will be inserted by the editor)

Event-triggered adaptive fault estimation and fault-tolerant control for strict-feedback nonlinear systems with full state constraints

Ming-Rui Liu · Li-Bing Wu · Meng Wu · Wen-Chao Ma

Received: / Accepted:

Abstract This paper addresses the problem of event-based adaptive fault estimation (FE) and fault-tolerant control (FTC) for a class of strict-feedback nonlinear systems with full state constraints. The unknown fault and the to-be-tested states of the system are estimated by an innovative adaptive fault observer based on a modified intermediate variable update law with fault switching function. In addition, an event-triggered mechanism and adaptive fault-tolerant controller co-design scheme is proposed according to backstepping algorithm and constrained technique, which not only eliminates the effect of fault presence but also leads to a significant reduction of communication resources. Through theoretical analysis, the constructed controller ensures that all signals within the system are ultimately bounded, and the state errors converge to the desired neighborhoods. Finally, the effectiveness of the method is illustrated by a simulation example of a single-link robot system.

Ming-Rui Liu
School of Science, University of Science and Technology Liaoning, Anshan 114051, P. R. China.
E-mail: 16642299868@163.com

Li-Bing Wu (✉)
Department of Mathematics, School of Science, University of Science and Technology Liaoning, Anshan, Liaoning 114051, P. R. China.
E-mail: beyondwlb@163.com

Meng Wu
School of Science, University of Science and Technology Liaoning, Anshan 114051, P. R. China.
E-mail: beyondwm1105@163.com

Wen-Chao Ma
Mathematics Teaching and Research Group, Dongyuan Senior High School, Lanling County, Linyi, Shandong 277700, P. R. China.
E-mail: yoursmwc@163.com

Keywords Fault estimation · fault-tolerant control · event-triggered mechanism · full state constraints

1 Introduction

In real life, since system faults may lead to serious consequences, including the decline of mechanical performance, property damage and even the risk of life safety, fault detection and isolation technique [1]-[3] must be added to improve system safety and reliability in practical control operations. Nevertheless, it is still not enough to accurately capture the size and type of faults only by the means mentioned above. Fortunately, FE [4,5] can describe the details of fault information online and perform the required fault detection automatically. Because of this, many scholars have conducted in-depth research on it and achieved some important results. Currently, the main methods of FE are broadly categorized into: robust estimation observer [6], adaptive fault estimator [7], sliding mode observer[8], and intermediate variable-based estimation [9]. The last method is more effective in terms of estimation accuracy, and thus becomes the mainstream method of FE at present. For a class of nonlinear systems with faults, in [10], a lower triangular matrix-based observer structure design criterion was proposed to design a fault estimation observer with generally relaxed constraints. Furthermore, to address the mismatch phenomenon and the stochastic fault matter, a stochastic intermediate variable estimator was designed in [11] to estimate the states and faults simultaneously. It is worth noting that the above literature does not apply FTC, which can reduce the impact of faults on system performance. In fact, a combination of the two techniques would be more useful and meaningful while

dealing with strict-feedback nonlinear systems. For example, in [12], a fault-tolerance scheme based on intermediate variable was proposed for a class of nonlinear systems with unknown time-varying system faults and dead-zones. For multiple unmanned aerial vehicles [13] under the case of sensor faults and directed connective communication topology, a fixed-time fault-tolerance strategy was developed. Even further, to settle more complex systems, such as those containing uncertain nonlinear functions, an adaptive FE fuzzy state observer was designed in [14] to measure unknown states, nonlinear function terms, and a time-varying fault. Although some adaptive FE and FTC have made certain research advances, the aforementioned achievements do not take into account the constraint condition. If this case was ignored, it can lead to performance degradation in many real systems, such as robotic system [15], marine system [16], etc.

In fact, constraints widely exist in many practical systems and have become an important factor affecting the proper functioning of the system. In [17]-[20], various methods have been employed to cope with the constraint problems, among which the Barrier Lyapunov function (BLF) has been recognized and favored by many experts as an effective tool. In [21], for constrained MIMO uncertain nonlinear systems, an adaptive control scheme with symmetric constraint on output variable was proposed. In [22], an adaptive fuzzy tracking control scheme was developed for a class of uncertain nonlinear systems with partial state constraints and output dead-zones. Compared with the symmetric constraint, an adaptive control solution with asymmetric time-varying constraints was offered in [23] which greatly increased the flexibility of the design while ensuring that the states can be restricted to boundaries that change over time. Further, based on the nature of the constraints, the authors of [24] applied the constraint method to fault error and constructed a FE update law, which led to an improvement in the estimation accuracy and limited the fault error to a specified region, thus realizing FTC.

However, the signals from the controllers in the above references are transmitted cyclically, meaning that they are time-sampled, which results in a huge waste of resources, and to counter this, event-triggered control (ETC) technology [25,26] has attracted the attention of the crowd. Depending on the magnitude of the control input signal, three triggering strategies were designed in [27] to handle uncertain nonlinear systems. In [28], an adaptive fuzzy fixed-time tracking control problem based on event-triggered was investigated for systems with unknown control coefficients. Meanwhile, for a class of nonlinear systems with actuator faults, a triggered controller was proposed in [29] that not only made the communication burden from the controller to the actuator less burdensome, but also allowed the total number of faults to be infinite. When studying the fuzzy adaptive event-based problems for uncertain non-affine nonlinear systems, a tracking error reduction function was designed in [30], which effectively reduced the number of triggered. In addition, the work in [31] cited an event triggering containment controller to make multi-agent system resistant to denial-of-service attacks. Nevertheless, the aforesaid references still follow the triggering strategies of fixed threshold and relative threshold. At the same time, there are few works on FE and FTC based on event-triggered mechanism. Therefore, it has important theoretical and application significance to design an event-based adaptive fault estimation and fault-tolerant control scheme for strict feedback nonlinear systems with full state constraints.

For the content to be studied, there are several difficulties as follows:

1) How to improve the method of intermediate variable used in most of the literature related to fault estimation to make the modified scheme work even better;

2) Is it possible to follow the constraint on fault error in the previous works [24] and devise a more reasonable fault switching signal to make the design process simpler and more widely applicable?

3) Designing a necessary controller that simultaneously ensures system stability, achieves higher estimation accuracy, improves fault-tolerant tracking efficiency, and further reduces resource waste is a complex task.

Based on the above discussions, this paper investigates an event-based approach about fault estimation and fault-tolerant co-design for strictly feedback nonlinear systems. Compared to previous studies, the key contributions of this research are:

1) Different from the traditional intermediate variable approach [12,14], where the coefficient of x_n is a constant, we propose a more general intermediate variable way incorporating a time-varying function gain of x_n, which leads to a better fault estimation accuracy.

2) Compared with [24], an improved and more reasonable fault switching signal that contains fault supremum and infimum as well as estimated fault information is considered herein, which enhances the applicability for different fault signals.

3) Unlike References [4]-[14], a method about fault-tolerant control and event triggering mechanism co-design is presented by backstepping technique. Besides, in contrast with the relative threshold triggering strategy in [25] and [27], a novel triggered approach based on system characteristic is implemented to further reduce

the computational requirements of the communication process.

The other sections are arranged as follows:

Section 2 provides the system to be studied in this paper, some basic assumptions and control tasks. In Section 3, we propose an adaptive fault observer system as well as a fault estimator and provide the corresponding theoretical supports. In Section 4, we construct a design scheme for a fault-tolerant controller based on event triggering and provide a relevant proof of stability analysis. A simulation example of single-link robot under different fault signals is shown in Section 5 to validate the effectiveness of the design approach and the conclusion of the paper is given in Section 6.

2 Problem Formulations and preliminaries

Consider a class of nonlinear systems with time-varying actuator faults

$$\begin{aligned} \dot{x}_i &= x_{i+1}, \quad i = 1, \cdots, n-1 \\ \dot{x}_n &= gu + F(x) + \eta(t) \\ y &= x_1 \end{aligned} \tag{1}$$

where x_i, $i = 1, \cdots, n-1$, and x_n are system state vectors and all states are unknown except for x_1. $u \in \mathbb{R}$ and $y \in \mathbb{R}$ are the real control input and the measured output, in that order, g corresponds to a known control gain, $\eta(t)$ signifies the existence of a fault in the system that varies over time and is not known, $F(x) = \sum_{j=1}^{N} f_j(x)$ is smooth function that is already known, where $x = [x_1, x_2, \cdots, x_n]^T$, $j = 1, 2, \cdots, N$.

Control tasks: For strict-feedback nonlinear system (1), a novel adaptive fault estimator and event-based fault-tolerant controller are designed such that:

(1). All signals in a closed-loop system are uniformly and ultimately bounded.

(2). The system output y can effectively track the reference signal y_d, moreover, the other states of the system and their corresponding observed states are also well fitted.

(3). Fault error and other state errors are within predefined bounded compact sets.

Here are some necessary Assumptions:

Assumption 1 For the reference signal y_d, it is known to be bounded, and its i-th derivative $y_d^i, i = 1, \cdots, n$, is also bounded.

Assumption 2 The fault signal $\eta(t)$ is bounded, that is, there exists a known supremum and infimum such that it satisfies $\eta_l^* < \eta < \eta_u^*$. And its first-order derivative $\dot{\eta}(t)$ is also bounded, satisfying $\dot{\eta}(t) \leq \delta$, where δ is a known positive constant.

Assumption 3 The nonlinear function $f_j(x), j = 1, \cdots, N$, satisfies the Lipschitz continuity condition, that is, $|f_j(x) - f_j(\hat{x})| \leq L_j|x - \hat{x}|$, where L_j is Lipschitz constant. Let $L = \max_{1 \leq j \leq N}\{L_j\}$ and then we further obtain $|F(x) - F(\hat{x})| \leq NL|x - \hat{x}|$.

Remark 1 Assumptions 1 and 3 have been raised in literature [12,24] and are reasonable. For Assumption 2, it is reflected in many real-life examples, yet the fault is considered to be fluctuation within a certain range, for example, grid voltage fluctuations: voltage fluctuations in the power system are normal, but should be controlled within a certain range, too high or too low fluctuations can affect the operation of electronic equipment [34]; aircraft speed range: aircrafts have a maximum and minimum speed range, and exceeding these speed ranges may lead to structural damage, loss of control or unstable flight [35]; tire pressure range: car tires need to maintain a specific range of air pressure in order to operate properly, too low an air pressure may lead to increased tire wear, while too high an air pressure may affect the suspension system [36].

3 Adaptive Fault Estimator Design

In this section, we design an adaptive fault observer to estimate the system states as well as the unknown time-varying fault, simultaneously.

Consider the adaptive fault observer system:

$$\begin{aligned} \dot{\hat{x}}_i &= \hat{x}_{i+1} + l_i(y - \hat{x}_1), \quad i = 1, \cdots, n-1 \\ \dot{x}_n &= gu + F(\hat{x}) + \hat{\eta}(t) + l_n(y - \hat{x}_1) \\ \hat{y} &= \hat{x}_1 \end{aligned} \tag{2}$$

where $\hat{x}_i$ and $\hat{x}_n$, l_i and l_n, $i = 1, \cdots, n-1$, each represent the observations of the system states and the observer gains. $F(\hat{x})$ is the estimated value of $F(x)$, $\hat{\eta}(t)$ is the estimated value of the time-varying fault $\eta(t)$.

Since the fault is often unknown in real system, the corresponding fault error is not available. And if we want to introduce the constraint over the fault error [24], we need to first introduce the definition of the fault switching signal, which can be used to replace fault error, the expression for the fault switching signal is

$$\tilde{\eta}_0 = \begin{cases} \lambda \frac{\hat{\eta} - \eta_u^*}{\hat{\eta} - \eta_l^*}, & \text{if } \eta_u^* \leq \hat{\eta} \\ \min\left\{\lambda \frac{\hat{\eta} - \eta_l^*}{\eta_u^* - \eta_l^*}, \lambda \frac{\eta_u^* - \hat{\eta}}{\eta_u^* - \eta_l^*}\right\}, & \text{if } \eta_l^* < \hat{\eta} < \eta_u^* \\ \lambda \frac{\hat{\eta} - \eta_l^*}{\hat{\eta} - \eta_u^*}, & \text{if } \hat{\eta} \leq \eta_l^* \end{cases} \tag{3}$$

here λ is the adjustment factor, which satisfies $0 < \lambda \leq 1$.

In order to achieve the estimation of time-varying fault, we design a more general intermediate variable: $z = \eta - (p(t) + \gamma)x_n$, where $p(t)$ is a time-varying function that satisfies $\dot{p}(t) = -p(t)^2 - 2p(t)\gamma$, γ is a known normal number. Then we get the derivative of z

$$\dot{z} = \dot{\eta} - \dot{p}(t)x_n - (p(t) + \gamma)(gu + F(x) + z + (p(t) + \gamma)x_n) \tag{4}$$

Furthermore, according to the definition of $\dot{z}$ in (4), the intermediate variable update law is designed to

$$\dot{\hat{z}} = -\dot{p}(t)\hat{x}_n - (p(t) + \gamma)(gu + F(\hat{x}) + \hat{z} + (p(t) + \gamma)\hat{x}_n) + C \tag{5}$$

in which C is the fault switching function associated with the failover signal, denoted by

$$C = \frac{\tilde{\eta}_0}{K_f^2 - \tilde{\eta}_0^2} + \tau_0\tilde{\eta}_0 \tag{6}$$

therein K_f and τ_0 we will give later.

According to $z = \eta - (p(t) + \gamma)x_n$, the estimate of the unknown time-varying fault $\eta(t)$ can be written as

$$\hat{\eta} = \hat{z} + (p(t) + \gamma)\hat{x}_n \tag{7}$$

This further yields the error between the fault and the estimated fault

$$\tilde{\eta} = \eta - \hat{\eta} \tag{8}$$

Define $\tilde{z} = z - \hat{z}$ and call (4) and (5) to generate the derivative of $\tilde{z}$

$$\dot{\tilde{z}} = \dot{\eta} - \dot{p}(t)e_n - (p(t) + \gamma)(F(x) - F(\hat{x}) + \tilde{z} + (p(t) + \gamma)e_n) - C \tag{9}$$

Remark 2 Since the fault error is not available, a fault switching signal is designed where this signal contains the supremum and infimum of the fault as well as its estimated value. According to (3), we can clearly see that a similar normalization approach is taken such that the switching signal $\tilde{\eta}_0$ is within the interval $[0, 1]$ in three different cases. From this we get $\tilde{\eta}_0 < \tilde{\eta}$, which leads to superior estimation accuracy. For detailed results, please refer to Figs. 6 and 7 in the simulation section.

Remark 3 Compared with the selection of $e_{f\delta}$ in [24], the formula for our switching signal is available and the value of it is not selected based on the true value of the actual fault, so the design of the fault switching signal in this paper is more reasonable. In addition, it can be easily seen that whether it is the design of the fault switching signal (3), the selection of the intermediate variable update law (5), or the construction of fault estimator (7), References [12,14,24] are special cases of our design method.

Defining the observation error as $e = x - \hat{x}$, the derivative of observation error can be obtained from equation (1) and equation (2) as

$$\dot{e} = Ae + B_n\left(F(x) - F(\hat{x}) + \tilde{\eta}\right) \tag{10}$$

with

$$A = \begin{bmatrix} -l_1 & 1\ 0 \dots 0 \\ -l_2 & 0\ 1 \dots 0 \\ \vdots & \vdots\ \vdots\ \ddots\ \vdots \\ -l_{n-1} & 0\ 0 \dots 1 \\ -l_n & 0\ 0 \dots 0 \end{bmatrix},\ B_n = \begin{bmatrix} 0 \\ 0 \\ \vdots \\ 1 \end{bmatrix} \tag{11}$$

where l_i is chosen such that A is a Hurwitz matrix. Thus, for a given matrix $Q = Q^T > 0$, there exists a matrix $P = P^T > 0$ that satisfies

$$A^T P + PA = -2Q \tag{12}$$

Lemma 1 *Assuming $\delta^* > 0$ is an unchanging positive quantity and α is any real number, the following inequality is valid:*

$$0 \leq |\alpha| - \alpha \tanh\left(\frac{\alpha}{\delta^*}\right) \leq \kappa\delta^* \tag{13}$$

where $\kappa = \sup_{\nu>0}\{\frac{\nu}{1+e^{\nu}}\} = 0.2785$.

Lemma 2 *$f(x) = \frac{x^2}{K^2 - x^2}$ and $g(x) = \frac{x^2}{(K^2 - x^2)^2}$ are continuous functions and [a,b] is their closed interval, then there exists x_0 such that $|f(x) - f(x_0)| = \epsilon_1^*$ and $|g(x) - g(x_0)| = \epsilon_2^*$holds, respectively. Where K is a designed boundary making $|x| < K$ hold, $\epsilon_1^* > 0$ and $\epsilon_2^* > 0$ are bounded constants.*

Remark 4 Lemma 1 is very common in event-triggered related articles [30,37], and Lemma 2 applies the related definition that continuous functions are bounded in closed intervals.

Lemma 3 *According to the fault switching signal* (3)*, the intermediate variable update law* (5)*, the fault estimator* (7) *and the error system* (10)*, the fault error $\tilde{\eta}$ is guaranteed to be uniformly ultimately bounded (UUB) under the above Assumptions* 1-3*, and Lemma* 2*.*

Proof: Consider the Lyapunov function associated with the state error e, the intermediate variable error $\tilde{z}$ and the fault error $\tilde{\eta}$ to be

$$V_0 = \frac{1}{2}e^T Pe + \frac{1}{2}\log\frac{K_f^2}{K_f^2 - \tilde{\eta}^2} + \frac{1}{2}\tilde{z}^2 \tag{14}$$

According to equation (3) we have $\tilde{\eta}_0 < |\tilde{\eta}| < K_f$, where K_f is a predesigned bounded compact set. The derivative of V_0 is

$$\begin{aligned}\dot{V}_0 &= \frac{1}{2}e^T(A^TP+PA)e + e^TPB_n(F(x)-F(\hat{x})) \\ &+ e^TPB_n\tilde{\eta} + \frac{\tilde{\eta}(\dot{\eta}-\dot{\hat{\eta}})}{K_f^2-\tilde{\eta}^2} + \tilde{z}(\dot{\eta}-\dot{p}(t)e_n-(p(t)+\gamma) \\ &(F(x)-F(\hat{x})+\tilde{z}+(p(t)+\gamma)e_n)-C)\end{aligned} \tag{15}$$

The inequalities are deflated to show that

$$\begin{aligned} e^TPB_n(F(x)-F(\hat{x})) &\le NL\|P\|\|e\|^2 \\ e^TPB_n\tilde{\eta} &\le \frac{1}{2}\|P\|^2\|e\|^2+\tilde{z}^2+(p(t)+\gamma)^2\|e\|^2 \\ \frac{\tilde{\eta}(\dot{\eta}-\dot{\hat{\eta}})}{K_f^2-\tilde{\eta}^2} &\le \frac{-\tau_0\tilde{\eta}^2}{K_f^2-\tilde{\eta}^2}+\epsilon_2^*+\frac{\delta^2}{2}+\tau_0\epsilon_1^*+\frac{1}{2}(p(t)+\gamma)^2l_n^2\|e\|^2 \\ -\tilde{z}(p(t)+\gamma)^2e_n &\le -\tilde{z}p^2(t)e_n-2p(t)\gamma\tilde{z}e_n+\frac{1}{2}\gamma^4\|e\|^2+\frac{1}{2}\tilde{z}^2 \\ -\tilde{z}\dot{p}(t)e_n &= p^2(t)\tilde{z}e_n+2p(t)\gamma\tilde{z}e_n \\ -\tilde{z}(p(t)+\gamma)(F(x)-F(\hat{x})) &\le \tilde{z}^2+\frac{N^2L^2\left(p^2(t)+\gamma^2\right)}{2}\|e\|^2 \\ \tilde{z}\dot{\eta} &\le \frac{1}{2}\tilde{z}^2+\frac{1}{2}\delta^2 \end{aligned} \tag{16}$$

Substituting (16) into equation (15) yields

$$\dot{V}_0 \le -P_0\|e\|^2-(p(t)+\gamma-3)\,\tilde{z}^2-\frac{\tau_0\tilde{\eta}^2}{K_f^2-\tilde{\eta}^2}+D_0 \tag{17}$$

where $P_0=\lambda_{\min}(Q)-NL\|P\|-\frac{1}{2}\|P\|^2-(p(t)+\gamma)^2-\frac{N^2L^2(p^2(t)+\gamma^2)}{2}-\frac{1}{2}\gamma^4-\frac{1}{2}(p(t)+\gamma)^2l_n^2$, $D_0=\delta^2+\epsilon_2^*+\tau_0\epsilon_1^*$, in which $\tau_0>0$ is a normal number. Next, depending on $\log\frac{K_f^2}{K_f^2-\tilde{\eta}^2}<\frac{\tilde{\eta}^2}{K_f^2-\tilde{\eta}^2}$ and rationalizing the parameters used above, we can conclude that $\tilde{\eta}$ is UUB. This proof is complete.

4 Event-based Adaptive fault-tolerant tracking controller design

In this section, for the nonlinear system with time-varying fault (1), we design an event-based adaptive FTC scheme by backstepping and constrained methods. Firstly, the corresponding coordinate transformations:

$$\begin{aligned} z_1 &= x_1-y_d, \\ z_i &= \hat{x}_i-\alpha_{i-1},\ i=2,\dots,n \end{aligned} \tag{18}$$

where y_d is a reference signal to be tracked, α_{i-1} is the virtual control law in the subsequent $n-1$ steps.

Step 1: Initial, the derivation of z_1 yields

$$\begin{aligned}\dot{z}_1 &= x_2-\dot{y}_d \\ &= e_2+z_2+\alpha_1-\dot{y}_d\end{aligned} \tag{19}$$

In order to ensure that the system state is not violated, BLF is used

$$V_1 = V_0+\frac{1}{2}\log\left(\frac{K_1^2}{K_1^2-z_1^2}\right) \tag{20}$$

where K_1 is a compact set to be designed and meets the $\Omega_{z_1}=\{|z_1|<K_1\}$.

Derivating for (20) and substituting (17) yields

$$\begin{aligned}\dot{V}_1 &= -P_0\|e\|^2-(p(t)+\gamma-3)\tilde{z}^2-\frac{\tau_0\tilde{\eta}^2}{K_f^2-\tilde{\eta}^2} \\ &+ D_0+\frac{z_1(e_2+z_2+\alpha_1-\dot{y}_d)}{K_1^2-z_1^2}\end{aligned} \tag{21}$$

Using Young's inequality to deflate the following equations yields

$$\begin{aligned}\frac{z_1e_1}{K_1^2-z_1^2} &\le \|e\|^2+\frac{1}{4}\frac{z_1^2}{(K_1^2-z_1^2)^2} \\ \frac{z_1z_2}{K_1^2-z_1^2} &\le z_2^2+\frac{1}{4}\frac{z_1^2}{(K_1^2-z_1^2)^2}\end{aligned} \tag{22}$$

Next we design the virtual control law α_1 as

$$\alpha_1 = -k_1z_1-\frac{1}{2}\frac{z_1}{K_1^2-z_1^2}+\dot{y}_d \tag{23}$$

where $k_1>0$ is a parameter of the design.

Substituting (22) and (23) into (21), $\dot{V}_1$ is

$$\begin{aligned}\dot{V}_1 &= -P_1\|e\|^2-(p(t)+\gamma-3)\tilde{z}^2-\frac{\tau_0\tilde{\eta}^2}{K_f^2-\tilde{\eta}^2} \\ &+ D_0-\frac{k_1z_1^2}{K_1^2-z_1^2}+z_2^2\end{aligned} \tag{24}$$

where $P_1=P_0-1$.

Step 2: Derivation with respect to z_2 yields

$$\dot{z}_2 = \hat{x}_3+l_2(y-\hat{x}_1)+\dot{\alpha}_1 = z_3+\alpha_2+l_2(y-\hat{x}_1)-\dot{\alpha}_1 \tag{25}$$

Accordingly, the BLF is chosen to be

$$V_2 = V_1+\frac{1}{2}\log\left(\frac{K_2^2}{K_2^2-z_2^2}\right) \tag{26}$$

Derivation on (26) yields

$$\dot{V}_2 = \dot{V}_1+\frac{z_2(z_3+\alpha_2+l_2(y-\hat{x}_1)-\dot{\alpha}_1)}{K_2^2-z_2^2} \tag{27}$$

Introducing the following inequality deflation

$$\frac{z_2 z_3}{K_2^2 - z_2^2} \leq z_3^2 + \frac{1}{4}\frac{z_2^2}{(K_2^2 - z_2^2)^2} \tag{28}$$

The virtual control law α_2 is as follows

$$\alpha_2 = -k_2 z_2 - (K_2^2 - z_2^2)z_2 - \frac{1}{4}\frac{z_2}{K_2^2 - z_2^2} - l_2(y - \hat{x}_1) + \dot{\alpha}_1 \tag{29}$$

with $k_2 > 0$ is the design parameter, K_2 is a designed compact set and that it satisfies $\Omega_{z_2} = \{|z_2| < K_2\}$.

Substituting (24), (28) and (29), (27) is rewritten as

$$\begin{aligned}\dot{V}_2 = &-P_1\|e\|^2 - (p(t) + \gamma - 3)\tilde{z}^2 - \frac{\tau_0\tilde{\eta}^2}{K_f^2 - \tilde{\eta}^2} \\ &+ D_0 - \sum_{i=1}^{2}\frac{k_i z_i^2}{K_i^2 - z_i^2} + z_3^2\end{aligned} \tag{30}$$

Step i($3 \leq i \leq n-1$): Based on the above two steps we recursively obtain for the next step i.

$$\begin{aligned}\dot{V}_i = &-P_1\|e\|^2 - (p(t) + \gamma - 3)\tilde{z}^2 - \frac{\tau_0\tilde{\eta}^2}{K_f^2 - \tilde{\eta}^2} \\ &+ D_0 - \sum_{i=1}^{i}\frac{k_i z_i^2}{K_i^2 - z_i^2} + z_{i+1}^2\end{aligned} \tag{31}$$

In step i, the choice of the virtual control law α_i is

$$\alpha_i = -k_i z_i - (K_i^2 - z_i^2)z_i - \frac{1}{4}\frac{z_i}{K_i^2 - z_i^2} - l_i(y - \hat{x}_1) + \dot{\alpha}_{i-1} \tag{32}$$

where $k_i > 0$ is the parameter to be designed, K_i is a designed compact set and it fulfills $\Omega_{z_i} = \{|z_i| < K_i\}$.

Step n: In this step the actual control input will be designed, and we choose the last step of the coordinate transformation as follows

$$z_n = \hat{x}_n - \alpha_{n-1} \tag{33}$$

The derivative of z_n is

$$\dot{z}_n = gu + F(\hat{x}) + \hat{\eta} + l_n(y - \hat{x}_1) - \dot{\alpha}_{n-1} \tag{34}$$

We then construct the final step of the BLF as

$$V_n = V_{n-1} + \frac{1}{2}\log\left(\frac{K_n^2}{K_n^2 - z_n^2}\right) \tag{35}$$

After combining (31), the derivative of V_n is

$$\begin{aligned}\dot{V}_n \leq &-P_1\|e\|^2 - (p(t) + \gamma - 3)\tilde{z}^2 - \frac{\tau_0\tilde{\eta}^2}{K_f^2 - \tilde{\eta}^2} + D_0 - \sum_{i=1}^{n-1}\frac{k_i z_i^2}{K_i^2 - z_i^2} \\ &+ \frac{z_n\left((K_n^2 - z_n^2)z_n + gu + F(\hat{x}) + \hat{\eta} + l_n(y - \hat{x}_1) - \dot{\alpha}_{n-1}\right)}{K_n^2 - z_n^2}\end{aligned} \tag{36}$$

The control law for the nth step is

$$\alpha_n = -k_n z_n - (K_n^2 - z_n^2)z_n - F(\hat{x}) - \hat{\eta} - l_n(y - \hat{x}_1) + \dot{\alpha}_{n-1} \tag{37}$$

with $k_n > 0$ is a customizable positive element, K_n is a designed compact set and it fulfills $\Omega_{z_n} = \{|z_n| < K_n\}$.

Accordingly, to minimize the waste of communication resources, we use the following event triggering strategy

$$\begin{aligned}v(t) = &\, g^{-1}(1 + \delta_0)(\alpha_n - \delta_2 \tanh(\frac{z_n\delta_2}{\delta_1(K_n^2 - z_n^2)}) \\ &- g_0 \tanh(\frac{z_n g_0}{\delta_1(K_n^2 - z_n^2)}))\end{aligned} \tag{38}$$

$$\begin{aligned}&u(t) = v(t_s), \forall t \in [t_s, t_{s+1}), \\ &t_{s+1} = \inf\{t \in \mathbb{R}^+ | |e_u(t)| \geq \delta_0|u(t)| + \lambda_0 g_0(t) + \tau_1\}\end{aligned} \tag{39}$$

whereby $e_u(t) = v(t) - u(t)$ indicates the error arising from control sampling, g_0 is a function of the fault switching signal and satisfies $g_0 = \frac{1}{\frac{|\bar{\eta}_0|}{\Delta} + \kappa_0}$, $0 < \delta_0 < 1$, δ_1, δ_2, λ_0, τ_1, κ_0, Δ are all parameters to be designed, some of which satisfy the following inequality

$$\delta_0 < \delta_2,\ g\lambda_0 < 1 - \delta_0,\ g\tau_1 < \delta_2(1 - \delta_0) \tag{40}$$

The t_s, $s \in \mathbb{N}^+$ represents the triggering moment, i.e., when equation (39) is satisfied, it means that the trigger starts to activate, the time is changed from t_s to t_{s+1}, and the corresponding control signal $u(t_s)$ is changed to $u(t_{s+1})$. For $\forall t \in [t_s, t_{s+1})$, the control input signal always takes a constant value $v(t_s)$.

Remark 5 Inspired by [22], we add a function g_0 related to the fault switching signal to the triggering strategy. Compared with the triggering strategy with relative thresholds in [27], the addition of g_0 leads to a decrease in the number of times triggered, which further reduces the communication resources in the channel. Specific comparison results are later given by Table 1.

From (39), when $t \in [t_s, t_{s+1})$, we can deduce that $|e_u(t)| = |v(t) - u(t)| \leq \delta_0|u(t)| + \lambda_0 g_0 + \tau_1$. In place of absolute value as well as inequalitie, we devise a continuous function $c_0(t)$ such that $c_0(t_s) = 0$, $c_0(t_{s+1}) = \pm 1$, $|c_0(t)| \leq 1$.

It is not hard to deduce that

$$v(t) - u(t) = c_0(t)\left(\delta_0|u(t)| + \lambda_0 g_0 + \tau_1\right) \tag{41}$$

By transformation, we further obtain

$$u(t) = \frac{v(t) - c_0\tau_1 - c_0\lambda_0 g_0}{1 + c_1\delta_0} \tag{42}$$

where $c_1 = \pm c_0$, and also satisfies $|c_1| \leq 1$.

According to (38) and (40), we know that

$$\begin{aligned}\frac{z_n g v(t)}{(K_n^2 - z_n^2)(1 + c_1\delta_0)} &\leq \frac{z_n g v(t)}{(K_n^2 - z_n^2)(1 + \delta_0)} \\ &= \frac{z_n\left(\alpha_n - \delta_2 \tanh\left(\frac{z_n\delta_2}{\delta_1(K_n^2 - z_n^2)}\right) - g_0 \tanh\left(\frac{z_n g_0}{\delta_1(K_n^2 - z_n^2)}\right)\right)}{K_n^2 - z_n^2}\end{aligned} \tag{43}$$

Combined with Lemma 1, (38), and (41)-(43), (36) can be further written as

$$\begin{aligned}\dot{V}_n = &-P_1\|e\|^2 - (p(t) + \gamma - 3)\tilde{z}^2 - \frac{\tau_0\tilde{\eta}^2}{K_f^2 - \tilde{\eta}^2} + D_1 \\ &- \sum_{i=1}^{n} \frac{k_i z_i^2}{K_i^2 - z_i^2}\end{aligned} \tag{44}$$

where $D_1 = D_0 + 0.557\delta_1$.

A different representation of P_1 in (44) is given by

$$P_1 = Q - \beta I_{n\times n} \tag{45}$$

where $\beta = NL\|P\| + \frac{1}{2}\|P\|^2 + (p(t)+\gamma)^2 + \frac{N^2L^2(p^2(t)+\gamma^2)}{2} + \frac{1}{2}\gamma^4 + \frac{1}{2}(p(t)+\gamma)^2 l_n^2 + 1$.

Based on $\log\frac{K_i^2}{K_i^2 - z_i^2} < \frac{z_i^2}{K_i^2 - z_i^2}$, $i = 1, \ldots, n$ further we can get

$$\dot{V}_n = -\kappa_1 V + D_1 \tag{46}$$

where $\kappa_1 = \min\{\frac{\lambda_{\min}(Q - \beta I_{n\times n})}{\lambda_{\max}(P)}, 2(p(t)+\gamma-3), 2\tau_0, 2k_i, (i = 1, \ldots, n)\}$.

Theorem 1 *Consider the nonlinear system with time-varying actuator fault under Assumptions 1-3 subject to the constant constraints, based on our designed fault switching signal* (3)*, intermediate variable update law* (5)*, fault estimator* (7)*, fault switching function C, virtual control laws* (23)*,* (29)*,* (32)*,* (37)*, and designed event-triggered strategies* (38) *and* (39)*, the following conclusions are available:*

1) All states of the system are restricted to appropriate compact sets.

2) All signals in the closed-loop remain bounded.

3) The inter-execution interval $\{t_{s+1} - t_s\}$ *is lower bounded by a positive constant* T^**, where any s belongs to* $\mathbb{N}^*$*.*

4) The system's error signals are limited, and the following inequality holds:

$$\Omega_{z_i} = \{z_i | z_i| \ \leq K_i\sqrt{1 - e^{-\left(2V_n(0) + \frac{2D_1}{\kappa_1}\right)}}\} \tag{47}$$

Proof: By acting on both sides simultaneously $e^{\kappa_1 t}$ and then integrating $[0, t)$ over it, we get

$$V_n(t) \leq \left(V_n|_{t=0} - \frac{D_1}{\kappa_1}\right)e^{-\kappa_1 t} + \frac{D_1}{\kappa_1} \leq V_n(0) + \frac{D_1}{\kappa_1} \tag{48}$$

Based on (48) and a similar analytical procedure as in [22], we can conclude that all signals in the system are bounded and all states are at any time in suitable compact sets which satisfy $\Omega_{x_i} = \{x_i | x_i| \ \leq C_i\}$, $i = 1, \ldots, n$. It follows that the proof of conclusions 1) and 2) is complete.

Combining (35) and (48), we get

$$\frac{1}{2}\log\frac{K_i^2}{K_i^2 - z_i^2} \leq V_n(0) + \frac{D_1}{\kappa_1} \tag{49}$$

From the above equation it is easy to see that

$$|z_i| \leq K_i\sqrt{1 - e^{-\left(2V_n(0) + \frac{2D_1}{\kappa_1}\right)}} \tag{50}$$

Conclusion 4) stands.

Next, according to $e_u(t) = v(t) - u(t)$, and by taking the derivative of e_u, we can obtain the following inequality

$$|\dot{e}_u(t)| = |\dot{v}(t) - \dot{u}(t)| \leq |\dot{v}(t)| \tag{51}$$

Notice that looking at the expression for (38), we can clearly see that $v(t)$ is smooth-conductible, and by the smooth-conductible property, we see that there exists a constant V^* such that $v(t) < V^*$ holds. Thanks to $e_u(t_s) = 0$ and $\lim_{t\to t_{s+1}} e_u(t) = \delta_0|u(t)| + \lambda_0 g_0(t) + \tau_1$, it can be obtained that the lower bound of inner-event interval T^* meets $T^* \geq \frac{\delta_0|u(t)| + \lambda_0 g_0(t) + \tau_1}{V^*} \geq \frac{\tau_1}{V^*}$, So conclusion 3) is proved and according to conclusion 3), we know that Zeno behavior is cancel out.

In summary, the proof of Theorem 1 is complete.

Remark 6 Based on the above assumptions and lemmas, a novel approach to event-triggered adaptive FE and FTC of strict-feedback nonlinear systems with full state constraints is demonstrated. As a result, the designed fault switching signal (3), intermediate variable update law (5), fault estimator (7), and trigger strategies (38), (39) not only ensure that the fault signal can be well compensated, all the states of the closed-loop system do not violate the constraint boundaries, and the system state errors can converge to the desired neighborhoods of the origin, but also significantly reduce the computational burden of the communication process.

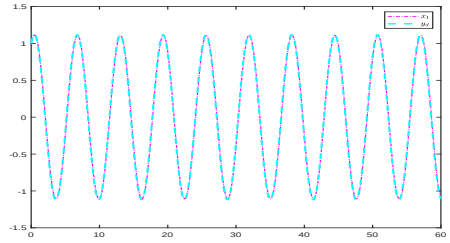


Fig. 1 Response curves of the system state x_1 and the reference signal to be tracked y_d.

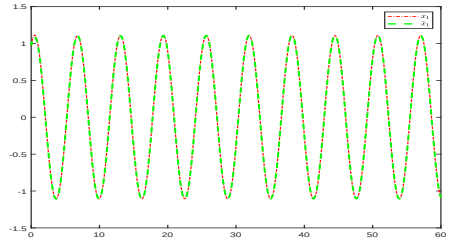


Fig. 2 The response curves of the system state x_1 and its estimated $\hat{x}_1$.

5 Simulation results

This part of the article will demonstrate the success of the proposed adaptive control mechanism using two different types of fault signals in the same simulation example.

Consider a single-link robot system with unknown time-varying fault in [24], whose expression is as follows:

$$\begin{aligned} \dot{x}_1 &= x_2 \\ \dot{x}_2 &= gu + F(x) + \eta \\ y &= x_1 \end{aligned} \tag{52}$$

where x_1 stands for the angle position q and x_2 stands for the angle velocity $\dot{q}$. $F(x) = f_1 + f_2$, among others $f_1 = -\frac{1}{2M}mgl\sin(x_1)$, $f_2 = -0.5e^{-2t}\cos(x_1x_2^2)$, the reference signal to be tracked we choose as $y_d = \cos(t) + 0.5\sin(t)$.

Case 1, the first fault signal we choose to be in the form of a segmented function expressed as follows

$$\eta = \begin{cases} 0.1t, & \text{if } 0 \le t < 5, \\ 0.06t - 0.3, & \text{if } 5 \le t < 35, \\ 1.8, & \text{if } 35 \le x \le 60. \end{cases} \tag{53}$$

The corresponding parameters of the actual single-link robot system are expressed as $m = 1kg$, $M = 0.5kgm^2$, $g = 9.8m/s^2$ and $l = 1m$. The parameters designed in the derivation are $l_1 = 20$, $l_2 = 35$, $k_1 = 10$, $k_2 = 25$, $K_1 = 0.1$, $K_2 = 0.1$, $\gamma = 3$, $\tau_0 = 0.001$, $K_f = 2.5$, $g = \frac{1}{M}$, $\lambda = 0.6$. The event-triggered related

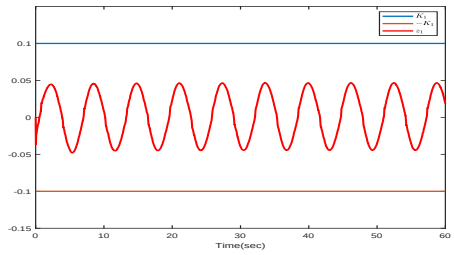


Fig. 3 Response curves for the output error z_1 and the designed bounded compact set K_1.

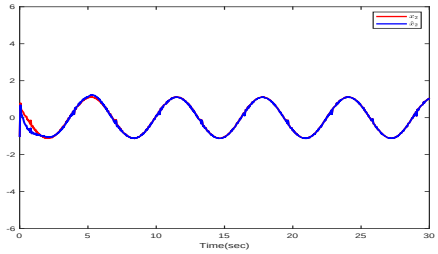


Fig. 4 The response curves of the system state x_2 and its estimated $\hat{x}_2$.

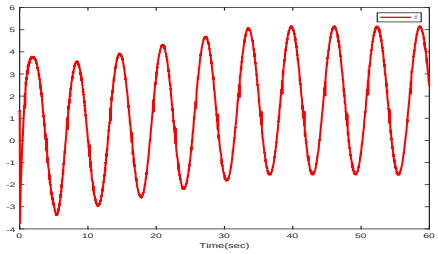


Fig. 5 Response curve for the estimate $\hat{z}$ of the intermediate variable z.

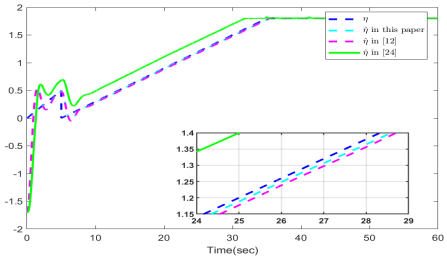


Fig. 6 Response curves of different estimation methods for segmented function type fault signal η.

parameters are designed as $\lambda_0 = 0.32$, $\delta_1 = 8$, $\delta_0 = 0.34$, $\delta_2 = 5$, $\tau_1 = 0.7$, $\kappa_0 = 5$. In addition we choose the initial values of the system to be $x_1(0) = 1$, $x_2(0) = -1$, $\hat{x}_1(0) = 1$, $\hat{x}_2(0) = -1$, $p(0) = 0$, $\hat{z}(0) = 1.3$.

Figs. 1-8 show plots of the results of simulation runs for this segmented type of fault signal. Figs. 1 and 2 show the tracking x_1 and y_d as well as the x_1 and its valuation $\hat{x}_1$ tracking curves, respectively. Fig. 3

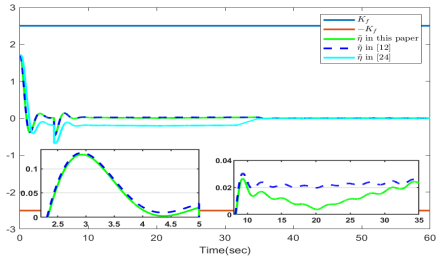


Fig. 7 Fault error response curves under different methods and the resulting bounded compact set K_f.

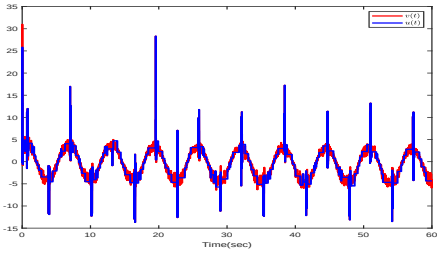


Fig. 8 Response curves for control inputs $v(t)$ and $u(t)$.

shows the curve of the output error z_1. Fig. 4 shows the tracking performance curves for x_2 and $\hat{x}_2$. From the above four figures, we can see that the designed control method leads to a good tracking performance of the system states. Figs. 5-7 show the plots related to fault. Fig. 5 illustrates the curve of the estimated value of the designed intermediate variable, which is bounded. As shown in Fig. 6, our designed fault estimation signal has more obvious tracking effect compared with the estimated signals in References [12,24]. Fig. 7 demonstrates the fault error curves of different methods, from which we can clearly see that the designed method makes the fault estimation error more accurate and closer to 0. In Fig. 8, it can be seen that both the control $u(t)$ and $v(t)$ are bounded.

Case 2, for the second fault signal we choose the form of sinusoidal signal, expressed as follows

$$\eta = 0.1\sin(t) \tag{54}$$

The designed system parameters, derivation parameters, triggered parameters and initial values of the system are the same as in the first case except for those shown later, which need to be changed: $\lambda_0 = 0.05$, $\delta_1 = 8.7$, $\tau_1 = 0.8$, $\kappa_0 = 11.7$.

Figs. 9-12 show the results of simulation run for a sinusoidal fault signal. As shown in Fig. 9, the estimate of the designed intermediate variable is also bounded under sinusoidal fault signal. As illustrated in Fig. 10, our designed fault estimation signal has a more accurate tracking effect compared with the estimation signal designed by the method in [24]. Fig. 11 shows the

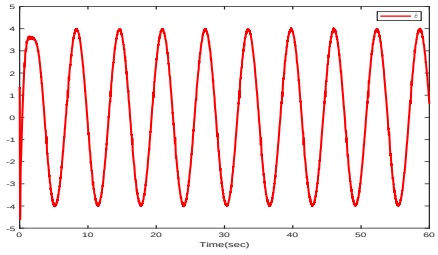


Fig. 9 Response curve of the estimated value $\hat{z}$ of the intermediate variable z under the second fault signal.

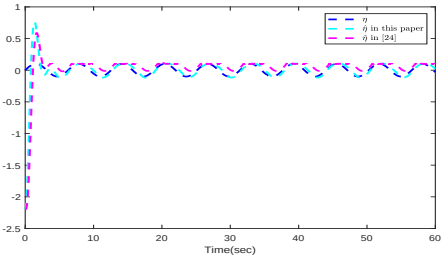


Fig. 10 Response curves for different estimation methods of the sinusoidal fault signal η.

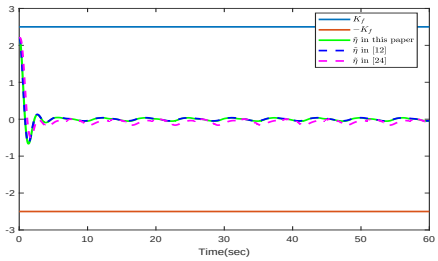


Fig. 11 Response curves of sinusoidal fault errors under different methods and the resulting bounded compact set K_f.

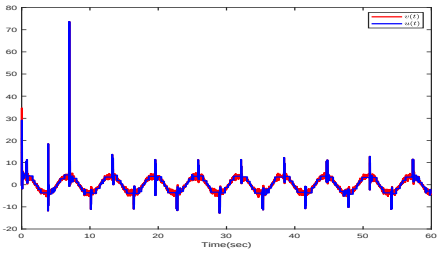


Fig. 12 Response curves of control inputs $v(t)$ and $u(t)$ under the second fault signal.

fault error curves of different methods under sinusoidal fault signal, from which we can obviously see that the proposed scheme makes the fault estimation error more precise. In Fig. 12, it can be seen that both the control signals $u(t)$ and $v(t)$ are bounded under the event-triggered control.

Table 1 Comparison of the number of different event triggering methods

Methods	Relative threshold	Proposed Threshold
Case 1	360	348
Case 2	366	334

Remark 7 Both under segmented function type fault signal and sinusoidal type fault signal, our designed event-triggered adaptive FE and FTC method can ensure that all the signals of the closed-loop system are bounded, the states of the system, as well as their respective estimated states, are well fitted, and the state errors are all within the designed bounded compact sets. For segmented function type fault signal, by comparing the improved fault switching signal designed in this paper with the methods in [12, 24], we can easily see that the designed method tracks better, with higher accuracy and smaller error. For sinusoidal fault signal, compared with the method in Reference [24] which cannot track the fault signal well and the fault error is large, our designed FE method overcomes this defect very well.

Remark 8 Throughout the entire text, we can clearly conclude that the constructed strategy not only has a more general design, wider application range, and better simulation results, but also is more in line with the actual design background. Although from Fig. 6 and Fig. 7 that our accuracy has not improved significantly, only around 0.01, in reality there are a lot of design systems with very high requirements for accuracy, and even if the accuracy is improved by about 0.01, it will bring remarkable optimization effects, for example, navigation systems: navigation systems are used to determine the position, direction, and trajectory of the movement. In applications such as the Global Positioning System (GPS), improving accuracy helps to pinpoint the position, especially in specific environments or remote areas where navigation is required, even a small improvement in accuracy can lead to more accurate positioning and navigation results; communication systems: radio and fiber optic communications and other fields require high accuracy, even if the accuracy is increased by 0.01 or so, it can also increase the channel capacity, reduce the BER, improve signal clarity.

6 Conclusion

In this thesis, an event-triggered adaptive FE and FTC scheme is developed for strict-feedback nonlinear systems. By designing a fault switching signal for replacing and reducing the fault error, we introduce a fault switching function, and then construct a more general intermediate variable update law to further improve the estimation accuracy. Moreover, the backstepping and constraint techniques are fully utilized to co-design the adaptive fault-tolerant tracking controller and event-triggering mechanism, which not only maintains the system stability, but also reduces the waste of resources. Based on stability analysis, it can be concluded that all closed-loop signals are bounded, fault error and system state errors converge to their respective bounded compact sets. The final simulation results proved the validity of this approach. In future work, we will consider the problem of event-triggered adaptive FE and FTC for nonlinear systems with uncertain term functions and sensor faults.

Data availibility

Data sharing not applicable to this article as no datasets were generated or analyzed during the current study

Compliance with ethical standards

The authors declare that they have no conflict of interest.

References

1. Quan, Y., Chen, W., Wu, Z.: Distributed fault detection and isolation for leader–follower multi-agent systems with disturbances using observer techniques. Nonlinear Dyn. 93, 863–871 (2018)
2. Hammouri, H., Kinnaert, M.: Observer-based approach to fault detection and isolation for nonlinear systems. IEEE Trans. Autom. Control 44(10), 1879-1884 (1999)
3. Kang, Y. F., Yao, L. N., W. W.: Sensor fault diagnosis and fault tolerant control for the multiple manipulator synchronized control system. ISA Trans. 106, 243-252 (2020)
4. Gao, Z. F., Wang, S.: Fault estimation and fault tolerance control for spacecraft formation systems with actuator fault and saturation. Optim. Control. Appl. Methods 42(6), 1591-1611 (2021)
5. Xie, X. P., Yue, D., Park, J. H.: Robust fault estimation design for discrete-time nonlinear systems via a modified fuzzy fault estimation observer. ISA Trans. 73, 22-30 (2018)
6. Rahimilarki, R., Gao, Z. W., Zhang, A. H., Binns, R.: Robust neural network fault estimation approach for nonlinear dynamic systems with applications to wind turbine systems. IEEE Trans. Ind. Inf. 15(12), 6302-6312 (2019)
7. Huang, S. J., Wu, L. B.: Adaptive estimation and output feedback FTC for nonlinear systems with unknown nonlinearities and faults. Int. J. Robust Nonlinear Control 28(17), 5297-5311 (2018)
8. Yang, H. Y., Yin, S.: Reduced order sliding mode observer-based fault estimation for Markov jump systems. IEEE Trans. Autom. Control 64(11), 4733-4740 (2019)

9. Liu, X. H., Han, J., Wei, X. J., Zhang, H. F., Hu, X.: Intermediate variable observer based fault estimation and fault-tolerant control for nonlinear stochastic system with exogenous disturbance. J. Franklin Inst. 357(9), 5380-5401 (2020)
10. Huang, S. J., Guo, L. D., Wu, L. B.: Fault estimation for nonlinear systems: an observer structure design criterion technique. Nonlinear Dyn. 110, 1651–1661 (2022)
11. Wang, G. L., Yi, C. L.: Fault estimation for nonlinear systems by an intermediate estimator with stochastic failure. Nonlinear Dyn. 89(2), 1195–1204 (2017)
12. Chen, M., Jiang, B., Guo, W. W.: Fault-tolerant control for a class of non-linear systems with dead-zone. Int. J. Syst. Sci. 47(7), 1689-1699 (2014)
13. Han, B., Jiang, J., Yu, C. J., Cao, T.: Distributed fault estimation and fixed-time fault-tolerant formation control for Multi-UAVs subject to sensor faults. J. Intell. Rob. Syst. 105(80), (2022)
14. Wu, Y., Zhang, G. S., Wu, L. B.: Observer-based adaptive fault estimation and fault-tolerant tracking control for a class of uncertain nonlinear systems. IET Control Theory Appl. 15, (2021)
15. He, W., Chen, Y., Yin, Z.: Adaptive neural network control of an uncertain robot with full-state constraints. IEEE Trans. Cybern. 46(3), 620-629 (2016)
16. He, W., Yin, Z., Sun, C. Y.: Adaptive neural network control of a marine vessel with constraints using the asymmetric Barrier Lyapunov function. IEEE Trans. Cybern. 47(7), 1641-1651 (2017)
17. Wang, M. M., Chai, Y., Luo, J.: A novel prescribed performance controller with unknown dead-zone and impactive disturbance. IEEE Access 8, 17160-17169 (2020)
18. Liu, C. G., Liu, X. P., Wang, H. Q., Zhou, Y. C., Lu, S. Y.: Finite-time adaptive tracking control for unknown nonlinear systems with a novel Barrier Lyapunov function. Inf. Sci. 528, 231-245 (2020)
19. Tee, K. P., Ge, S. S., Ren, B. B.: Control of nonlinear systems with time-varying output constraints. Automatica 47,(11) 2511-2516 (2011)
20. Liu, Y. J., Zhao, W., Liu, L., Li, D., Tong, S. C., Chen, C. L. P.: Adaptive neural network control for a class of nonlinear systems with function constraints on states. IEEE Trans. Neural Networks Learn. Syst. 34(6), 2732-2741 (2023)
21. Zhang, T. P., Liu, H. Q., Xia, M. Z., Yi, Y.: Adaptive neural control of MIMO uncertain nonlinear systems with unmodeled dynamics and output constraint. Int J Adapt Control Signal Process. 32(12), 1731-1747 (2018)
22. Liu, M. R., Wu, L. B., Yu, Q. K., Zhao. N. N.: Observer-based fuzzy adaptive event-triggered control for strictly uncertain nonlinear systems with partial state constraints and output dead-zones. Int. J. Syst. Sci. DOI: 10.1080/00207721.2023.2268778.
23. Liu, Y. J., Lu, S. M., Li, D. J., Tong, S. C.: Adaptive controller design-based ABLF for a class of nonlinear time-varying state constraint systems. IEEE Trans. Syst. Man Cybern.: Syst. 47(7), 1546-1553 (2017)
24. Wu, L. B., Wang, H., He, X. Q.: Adaptive fault estimation and fault-tolerant tracking control for a class of nonlinear systems with output constraints. IET Control Theory Appl. 12(4), 556-562 (2018)
25. Yang, P., Chen, X., Zhao, X.: Observer-based event-triggered tracking control for large-scale high order nonlinear uncertain systems. Nonlinear Dyn. 105, 3299–3321 (2021)
26. Hu, A., Park, J. H., Hu, M.: Consensus of nonlinear multiagent systems with intermittent dynamic event-triggered protocols. Nonlinear Dyn. 104(2), 1299-1313 (2021)
27. Xing, L. T., Wen, C., Liu, Z., Su, H., Cai, J.: Event-triggered adaptive control for a class of uncertain nonlinear systems. IEEE Trans. Autom. Control 62(4), 2071-2076 (2017)
28. Hu, X., Li, Y. X., Hou, Z.: Event-triggered fuzzy adaptive fixed-time tracking control for nonlinear systems. IEEE Trans. Cybern. 52(7), 7206-7217 (2022)
29. Xing, L. T., Wen, C. Y., Liu, Z. T., Su, H. Y., Cai, J. P.: Adaptive compensation for actuator failures with event-triggered input. Automatica 85, 129-136 (2017)
30. Wu, L. B., Park, J. H., Xie, X. P., Guo, C., Zhao, N. N.: Fuzzy adaptive event-triggered control for a class of uncertain nonaffine nonlinear systems with full state constraints. IEEE Trans. Fuzzy Syst. 29(4), 904-916 (2021)
31. Ma, Y. S., Che, W. W., Deng, C., Wu, Z. G.: Observer-based event-triggered containment control for MASs under DoS attacks. IEEE Trans. Cybern. 52(12), 13156-13167 (2022)
32. Ren, B. B., Ge, S. S., Tee, K. P., Lee, T. H.: Adaptive neural control for output feedback nonlinear systems using a Barrier Lyapunov function. IEEE Trans. Neural Networks 21(8), 1339-1345 (2010)
33. Zhang, L. L., Yang, G. H.: Fault-estimation-based output feedback adaptive FTC for uncertain nonlinear systems with actuator faults. IEEE Trans. Ind. Electron. 67(4), 3065-3075 (2020)
34. Hirase, Y., Abe, K., Sugimoto, K., Sakimoto, K., Bevrani, H., Ise, T.: A novel control approach for virtual synchronous generators to suppress frequency and voltage fluctuations in microgrids. Appl. Energy 210, 699-710 (2018)
35. Shen, Z. X., Tan, L., Yu, S. S., Song, Y. D.: Fault-tolerant adaptive learning control for quadrotor UAVs with the time-varying CoG and full-state constraints. IEEE Trans. Neural Networks Learn. Syst. 32(12), 5610-5622 (2021)
36. Liu, Y. J., Zeng, Q., Tong, S. C., Chen, C. L. P., Liu, L.: Adaptive neural network control for active suspension systems with time-varying vertical displacement and speed constraints. IEEE Trans. Ind. Electron. 66(12), 9458-9466 (2019)
37. Sun, J. K., Yang, J., Zeng, Z. G.: Predictor-based periodic event-triggered control for nonlinear uncertain systems with input delay. Automatica 136, 110055 (2022)